

# Overlapping Unit Cells in 3d Quasicrystal Structure

Helen Au-Yang and Jacques H.H. Perk

*Department of Physics, Oklahoma State University, 145 Physical Sciences,  
Stillwater, OK 74078-3072, USA*<sup>1</sup>

---

## Abstract

A 3-dimensional quasiperiodic lattice with overlapping unit cells is constructed using grid and projection methods pioneered by de Bruijn. Using Kronecker's theorem the frequencies of all possible types of overlapping are found.

*Key words:* Quasiperiodicity; pentagrid; Penrose tiles; overlapping unit cells.

---

Since the startling discovery of five-fold symmetry in quasiperiodic materials in 1984 [1], a great deal of research has been done on this subject by both physicists and mathematicians. Originally, quasicrystals were studied by filling the space aperiodically with nonoverlapping tiles, such as in Penrose tilings [2,3]. However, recently, Gummelt [5] motivated by physical considerations, proposed a description of quasicrystals in terms of overlappings of decagons. Further research [6,7,8,9] has shown that this may be a more sensible way to understand quasicrystalline materials—made of overlapping unit cells sharing atoms of nearby neighbors [7]. Here we use a multigrid method to produce a new example of 3-dimensional overlapping unit cells.

It is well-known that a Penrose tiling can be obtained by the projection of the 5-d euclidean lattice onto a particular 2-d cut-plane  $\mathcal{D}$  [4,10,11], and hence its diffraction pattern [12,13,14] has five- or ten-fold symmetry. It is also known that not all lattice points  $\mathbf{k}$  in  $\mathbb{Z}^5$  are allowed (in the sense that they can be mapped onto vertices of a Penrose tiling); only those points whose projections into the 3-dimensional orthogonal space  $\mathcal{W}$  are inside the window of acceptance [10,15] contribute. The window has been shown [10] to be the projection of the 5-d unit cell  $\text{Cu}(5)$  with  $2^5$  vertices into this 3-d space  $\mathcal{W}$ . Each facet shared by two neighboring 5-d unit cell cubes is 4-dimensional and when projected into 3-d space it produces a polyhedron  $\mathcal{K}$  with 12 faces. Therefore, the projections

---

<sup>1</sup> E-mail address: perk@okstate.edu .

of two adjacent 5-d unit cells into 3d must share a common projected facet  $\mathcal{K}$ . Thus the idea of overlapping decagons must have its extension to three dimension, by projecting the 5-d lattice into the space  $\mathcal{W}$ .

If  $\mathbf{d}_j$  are the generators of the plane  $\mathcal{D}$  and  $\mathbf{w}_j$  are the generators of its orthogonal space  $\mathcal{W}$ , then the projection operators are the matrices  $\mathbf{D}^T = (\mathbf{d}_0, \dots, \mathbf{d}_4)$  and  $\mathbf{W}^T = (\mathbf{w}_0, \dots, \mathbf{w}_4)$ , such that  $\mathbf{D}^T \mathbf{W} = \mathbf{W}^T \mathbf{D} = 0$ , where the superscript T denotes matrix transpose. More specifically, we choose

$$\mathbf{d}_j^T = (\cos j\theta, \sin j\theta), \quad \mathbf{w}_j^T = (\cos 2j\theta, \sin 2j\theta, 1) = (\mathbf{d}_{2j}^T, 1), \quad (1)$$

where  $j = 0, \dots, 4$  and  $\theta = 2\pi/5$ . Using notations and ideas introduced by de Bruijn [4], we consider the five grids consisting of bundles of equidistant planes defined by

$$x \cos 2j\theta + y \sin 2j\theta + z + \gamma_j = \mathbf{w}_j^T \mathbf{r} + \gamma_j = k_j, \quad (2)$$

for  $j = 0, \dots, 4$ ,  $k_j \in \mathbb{Z}$ . In (2),  $\mathbf{r}^T = (x, y, z)$ , and the  $\gamma_j$  are real numbers which shift the grids from the origin. We denote their sum by

$$\gamma_0 + \gamma_1 + \gamma_2 + \gamma_3 + \gamma_4 = c. \quad (3)$$

Without loss of generality, we may restrict  $c$  to  $c \leq 0 < 1$ .

It has been shown by de Bruijn [4] that the Penrose tiling associated with a 2-d pentagrid has simple matching rules only for  $c = 0$ . For  $0 < c < 1$  the corresponding generalized Penrose tilings do not satisfy simple matching rules, and have seven different sets of vertices corresponding to the different intervals of  $c$  [16]. Nevertheless, the diffraction patterns are believed to be the same for all values of  $c$  [17,18].

Let the integer  $k_j$  be assigned to all points sandwiched between the grid planes defined by  $k_j - 1$  and  $k_j$ . Then, five integers

$$K_j(\mathbf{r}) = \lceil \mathbf{w}_j^T \mathbf{r} + \gamma_j \rceil, \quad j = 0, \dots, 4, \quad (4)$$

(with  $\lceil x \rceil$  the smallest integer greater than or equal to  $x$ ), are uniquely assigned to every point  $\mathbf{r}$  in  $\mathbb{R}^3$ . A mesh in  $\mathbb{R}^3$  is now an interior volume, enclosed by grid planes, containing points with the same five integers. One next maps each mesh to a vertex in  $\mathcal{W}$  by

$$\mathbf{f}(\mathbf{r}) = \sum_{j=0}^4 K_j(\mathbf{r}) \mathbf{w}_j = \mathbf{W}^T \mathbf{K}(\mathbf{r}), \quad \mathbf{K}^T(\mathbf{r}) = (K_0(\mathbf{r}), \dots, K_4(\mathbf{r})). \quad (5)$$

The resulting collection of vertices  $\mathcal{L} = \{\mathbf{f}(\mathbf{r}) | \mathbf{r} \in \mathbb{R}^3\}$  is a 3-dimensional aperiodic lattice. It has been proven by de Bruijn [10], that a point  $\mathbf{k}$  in  $\mathbb{Z}^5$  satisfies the so-called *mesh condition* and therefore can be mapped into  $\mathcal{L}$  if and only if  $\mathbf{D}^T(\mathbf{k} - \boldsymbol{\gamma}) = \mathbf{D}^T\boldsymbol{\lambda}$ , where  $\boldsymbol{\gamma}^T = (\gamma_0, \dots, \gamma_4)$  and  $\boldsymbol{\lambda}^T = (\lambda_0, \dots, \lambda_4)$  with  $0 < \lambda_j < 1$  so that  $\boldsymbol{\lambda}$  is a point inside the 5-d unit cube  $\text{Cu}(5)$ . Thus, the *window of acceptance* is the interior of the convex hull of the points  $\mathbf{D}^T\mathbf{n}_i$ , where  $\mathbf{n}_i$  are the  $2^5$  vertices of the 5-d unit cube  $\text{Cu}(5)$ , see Fig. 1. We choose the 32  $\mathbf{n}_i$ 's as follows

$$\begin{aligned} \mathbf{n}_0 &= 0, & \mathbf{n}_{31} &= \mathbf{e}_0 + \mathbf{e}_1 + \mathbf{e}_2 + \mathbf{e}_3 + \mathbf{e}_4, \\ \mathbf{n}_{j+1} &= \mathbf{e}_{1-2j}, & \mathbf{n}_{j+6} &= \mathbf{e}_{1-2j} + \mathbf{e}_{4-2j}, & \mathbf{n}_{j+11} &= \mathbf{e}_{1-2j} + \mathbf{e}_{2-2j}, \\ \mathbf{n}_{j+16} &= \mathbf{e}_{1-2j} + \mathbf{e}_{2-2j} + \mathbf{e}_{5-2j}, & \mathbf{n}_{j+21} &= \mathbf{e}_{1-2j} + \mathbf{e}_{2-2j} + \mathbf{e}_{4-2j}, \\ \mathbf{n}_{j+26} &= \mathbf{e}_{1-2j} + \mathbf{e}_{2-2j} + \mathbf{e}_{4-2j} + \mathbf{e}_{5-2j}, & (j &= 0, \dots, 4), \end{aligned} \quad (6)$$

where  $\mathbf{e}_0, \dots, \mathbf{e}_4$  are the standard unit vectors in  $\mathbb{R}^5$ , with subscripts counted mod 5 ( $\mathbf{e}_j \equiv \mathbf{e}_{j \pm 5}$ ).

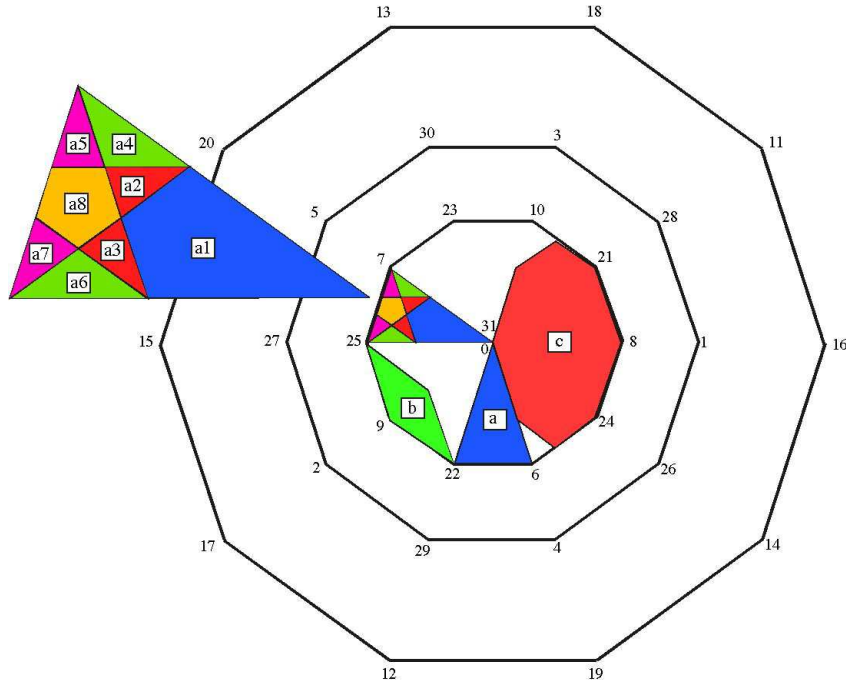


Fig. 1. The projection of the 5-d unit cube  $\text{Cu}(5)$  into the orthogonal 2d space  $\mathcal{D}$ . The window of acceptance is the interior of outer decagon  $\mathcal{Q}$  whose vertices are given by (9). The innermost decagon is denoted by  $\hat{\mathcal{Q}}$  and the middle decagon by  $\bar{\mathcal{Q}}$  with vertices given by (10). There are ten triangles of type (a), which are all further subdivided in eight regions of type (a1), ..., (a8), as is indicated for one case in the magnification on the left. This is determined by possible overlaps of this triangle with the ten regions each of types (b) and (c), see text.

The projection of Cu(5) with these 32 points into  $\mathcal{W}$  is a polytope  $\mathcal{P}$  with 40 edges connecting the 22 vertices, and with 20 faces. We let  $\mathbf{P}_i = \mathbf{W}^T \mathbf{n}_i$  for  $i = 0, \dots, 31$ . The bottom is  $\mathbf{P}_0 = (0, 0, 0)$  and top is  $\mathbf{P}_{31} = (0, 0, 5)$ ; they are called the tips of the polytope. The remaining twenty vertices of  $\mathcal{P}$  are

$$\begin{aligned} \mathbf{P}_{j+1} &= (\mathbf{d}_j, 1), & \mathbf{P}_{j+6} &= (\mathbf{d}_j + \mathbf{d}_{j+1}, 2), \\ \mathbf{P}_{j+21} &= (-\mathbf{d}_{j-2} - \mathbf{d}_{j-1}, 3), & \mathbf{P}_{j+26} &= (-\mathbf{d}_{j-1}, 4), \end{aligned} \quad (7)$$

for  $j = 0, \dots, 4$ . The other 10 points  $\mathbf{P}_{11}, \dots, \mathbf{P}_{20}$  are in the interior of the polytope and are given by

$$\mathbf{P}_{11+j} = (\mathbf{d}_j + \mathbf{d}_{j+2}, 2), \quad \mathbf{P}_{16+j} = (-\mathbf{d}_{j+1} - \mathbf{d}_{j-1}, 3), \quad (8)$$

again for  $j = 0, \dots, 4$ .

The orthogonal projection of Cu(5) into  $\mathcal{D}$  is a decagon  $\mathcal{Q}$  with 10 edges connecting the 10 vertices, see Fig. 1. Let  $\mathbf{Q}_i = \mathbf{D}^T \mathbf{n}_i$  for  $i = 0, \dots, 31$ . Then the vertices of the decagon are

$$\mathbf{Q}_{11+j} = -p\mathbf{d}_{3-2j}, \quad \mathbf{Q}_{16+j} = p\mathbf{d}_{5-2j}, \quad (9)$$

with  $j = 0, \dots, 4$ , and  $p = (\sqrt{5} + 1)/2$ . The remaining 22 points  $\mathbf{Q}_0, \dots, \mathbf{Q}_{10}$  and  $\mathbf{Q}_{21}, \dots, \mathbf{Q}_{31}$  are in the interior; they are given by

$$\begin{aligned} \mathbf{Q}_0 &= \mathbf{Q}_{31} = 0, & \mathbf{Q}_{j+1} &= \mathbf{d}_{5-2j}, & \mathbf{Q}_{26+j} &= -\mathbf{d}_{2-2j}, \\ \mathbf{Q}_{j+6} &= p^{-1}\mathbf{d}_{4-2j}, & \mathbf{Q}_{21+j} &= -p^{-1}\mathbf{d}_{3-2j}. \end{aligned} \quad (10)$$

Thus if the orthogonal projection  $\mathbf{D}^T(\mathbf{k} - \boldsymbol{\gamma})$  is in  $\mathcal{Q}$ , then its projection  $\mathbf{W}^T \mathbf{k}$  is in  $\mathcal{L}$ .

Consider a polytope  $\hat{\mathcal{P}}$  in  $\mathcal{L}$  whose bottom is the projection of a point  $\hat{\mathbf{k}}$  which is orthogonally projected onto the center of the decagon, then the ten vertices of  $\hat{\mathcal{P}}$  at height  $z = 1$  or  $z = 4$  correspond to the vertices of the middle decagon  $\bar{\mathcal{Q}}$ , see Fig. 1; the ten vertices of the polytope at height  $z = 2$  or  $z = 3$ , correspond to the vertices of the innermost decagon  $\hat{\mathcal{Q}}$ ; while the ten interior points of the polytope correspond to the vertices of the (outer) decagon  $\mathcal{Q}$  shown in Fig. 1.

Using an idea of de Bruijn [4], we may find out the condition for both  $\mathbf{k}$  and  $\mathbf{k} + \mathbf{n}_i$  to satisfy the mesh condition—to lie both in the window of acceptance.

It is straightforward to show that every point inside the innermost decagon  $\hat{\mathcal{Q}}$  corresponds to a point in  $\mathcal{L}$  that is connected with 10 neighbors, and is in fact

a tip of a polytope, as the middle decagon  $\bar{\mathcal{Q}}$  whose center is shifted to a point inside  $\hat{\mathcal{Q}}$  still lies inside  $\mathcal{Q}$ . This innermost decagon  $\hat{\mathcal{Q}}$  is further divided into 10 triangles. Whenever the center of a decagon  $\mathcal{Q}$  is shifted to a point inside one of the triangles, four of the vertices of the shifted outer decagon now lie inside  $\mathcal{Q}$ . More precisely, if  $\mathbf{D}^T(\mathbf{k} - \boldsymbol{\lambda})$  is inside triangle (a) in Fig. 1, then  $\mathbf{W}^T \mathbf{k}$  is a tip of a polytope  $\mathcal{P}$  whose interior points  $\mathbf{W}^T(\mathbf{k} + \mathbf{n}_{20})$ ,  $\mathbf{W}^T(\mathbf{k} + \mathbf{n}_{13})$ ,  $\mathbf{W}^T(\mathbf{k} + \mathbf{n}_{18})$  and  $\mathbf{W}^T(\mathbf{k} + \mathbf{n}_{11})$ —corresponding to the four points on  $\mathcal{Q}$  on the opposite side of triangle (a)—are now also in  $\mathcal{L}$ . This means each polytope in  $\mathcal{L}$  can have only four interior points which are also in  $\mathcal{L}$ . Thus each such unit cell contains 26 atoms, 22 exterior, and 4 interior sites.

It is also easy to find out how the polytopes share these interior points. This is equivalent to finding the condition that both  $\mathbf{k}$  and  $\mathbf{k} + \mathbf{n}_i$  for  $i = 1, \dots, 10$  or  $i = 21, \dots, 30$  are orthogonally projected into  $\hat{\mathcal{Q}}$ .

Consider the ten vertices of the polytope at height  $z = 1$  or  $z = 4$  corresponding to the vertices of middle decagon  $\bar{\mathcal{Q}}$ . When the center of the decagon is shifted to a point in one of ten rhombs of type (b) shown in Fig. 1, then one of the ten vertices of the shifted  $\bar{\mathcal{Q}}$  is inside  $\hat{\mathcal{Q}}$ . For the example in Fig. 1,  $\mathbf{W}^T(\mathbf{k})$  and  $\mathbf{W}^T(\mathbf{k} + \mathbf{n}_{28})$  are both tips of polytopes, with  $\mathbf{n}_{28}$  the point on  $\bar{\mathcal{Q}}$  on the opposite side of rhomb (b). As a consequence, the two polytopes share a polyhedron  $\mathcal{K}$  with 12 faces.

Moreover, the vertices of the polytope at  $z = 2$  or  $z = 3$  correspond to the vertices of  $\hat{\mathcal{Q}}$ . When the center of the decagon is shifted to a point in one of ten octagons of type (c) shown also in Fig. 1, then one of the ten vertices of the shifted  $\hat{\mathcal{Q}}$  moves inside  $\hat{\mathcal{Q}}$ . In Fig. 1  $\mathbf{W}^T(\mathbf{k})$  and  $\mathbf{W}^T(\mathbf{k} + \mathbf{n}_{25})$  are both tips of polytopes, while  $\mathbf{n}_{25}$  is the point on  $\hat{\mathcal{Q}}$  on the opposite side of the octagon. In this case, the two polytopes share a polyhedron  $\mathcal{J}$  with 6 faces.

By considering how these twenty regions intersect, we find that each of the triangles in  $\hat{\mathcal{Q}}$  is further divided into eight regions, as shown for one case in Fig. 1 with this triangle magnified on the left. When the orthogonal projection of  $\mathbf{k}$  is in (a1), its projection into  $\mathcal{W}$  is a polytope  $\mathcal{P}$  intersecting with four others whose tips are at  $\mathbf{W}^T(\mathbf{k} + \mathbf{n}_{21})$ ,  $\mathbf{W}^T(\mathbf{k} + \mathbf{n}_8)$ ,  $\mathbf{W}^T(\mathbf{k} + \mathbf{n}_{24})$  and  $\mathbf{W}^T(\mathbf{k} + \mathbf{n}_6)$ , and sharing with each of them a polyhedron of type  $\mathcal{J}$ . When the projection is in (a2) or (a3), either  $\mathbf{W}^T(\mathbf{k} + \mathbf{n}_{26})$  or  $\mathbf{W}^T(\mathbf{k} + \mathbf{n}_1)$  becomes also a tip of a polytope, so that  $\mathcal{P}$  intersects with five polytopes, sharing with one of them a polyhedron of type  $\mathcal{K}$ . In (a8),  $\mathcal{P}$  intersects with all of the above six polytopes. In regions (a5) or (a7),  $\mathbf{W}^T(\mathbf{k} + \mathbf{n}_{21})$  or  $\mathbf{W}^T(\mathbf{k} + \mathbf{n}_6)$  is no longer a tip and  $\mathcal{P}$  intersects with five polytopes sharing with two of them a polyhedron of type  $\mathcal{K}$ . Finally, while in (a4) or (a6), either  $\mathbf{W}^T(\mathbf{k} + \mathbf{n}_1)$  or  $\mathbf{W}^T(\mathbf{k} + \mathbf{n}_{26})$  is no longer a tip, and  $\mathcal{P}$  intersects with four polytopes sharing with one of them a polyhedron  $\mathcal{K}$  and with the other three a  $\mathcal{J}$ .

Therefore, there are only five different possibilities. The points inside a quadrilateral of type (a1) correspond to a polytope intersecting with four other polytopes sharing with each a polyhedron of type  $\mathcal{J}$ . This case is shown in Fig. 2a. Points inside triangles of type (a2) or (a3) correspond to a polytope intersecting with five other polytopes, sharing with one of them a polyhedron  $\mathcal{K}$  and with the other four polyhedra of type  $\mathcal{J}$ . Such a case is shown in Fig. 2b. If the point is inside triangles of type (a4) or (a6), the polytope intersects with four other polytopes sharing with one of them a polyhedron  $\mathcal{K}$  and with the other three polyhedra of type  $\mathcal{J}$ . If the point is in a triangle (a5) or (a7), the polytope intersects with five other polytopes sharing with two of them polyhedra of type  $\mathcal{K}$  and with the other three polyhedra  $\mathcal{J}$ . Finally, if the point is inside a pentagon (a8), the polytope intersects with six other polytopes sharing with two of them a  $\mathcal{K}$  and with the other four a  $\mathcal{J}$ . Their relative frequencies are related to the ratios of their areas and therefore the normalized probabilities are given by

$$\begin{aligned} P_{a1} &= 2p^{-3}, & P_{a2} = P_{a3} &= p^{-6}, & P_{a4} = P_{a6} &= p^{-5}, \\ P_{a5} &= P_{a7} = p^{-6}, & P_{a8} &= p^{-5} + p^{-7}. \end{aligned} \quad (11)$$

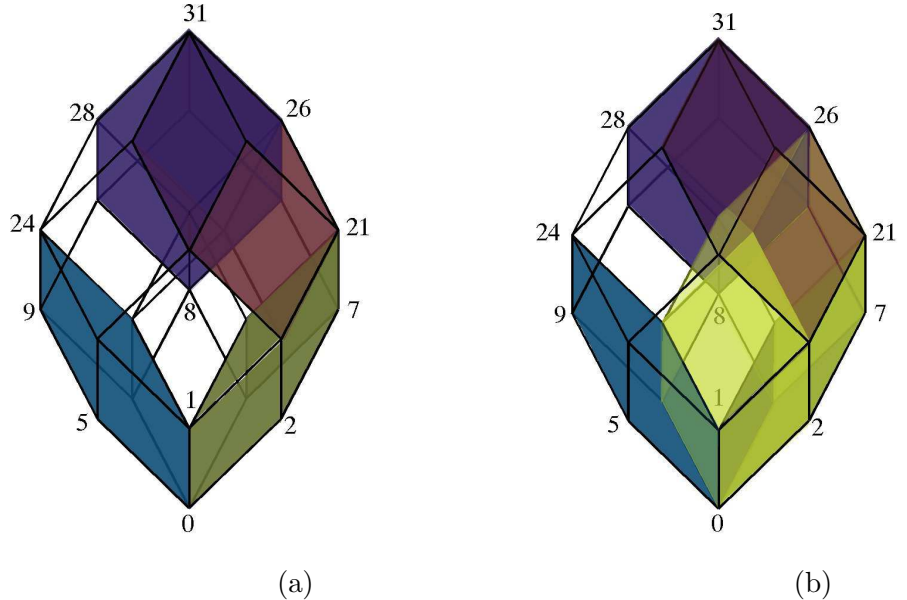


Fig. 2. (a) When the orthogonal projection of  $\mathbf{k}$  is in region (a1), its projection in  $\mathcal{L}$  is a polytope sharing an interior point with each of four neighboring polytopes whose tips are projections of  $\mathbf{k} + \mathbf{n}_{21}$ ,  $\mathbf{k} + \mathbf{n}_8$ ,  $\mathbf{k} + \mathbf{n}_{24}$  and  $\mathbf{k} + \mathbf{n}_6$ ; the shared interior points are projections of  $\mathbf{k} + \mathbf{n}_{11}$ ,  $\mathbf{k} + \mathbf{n}_{16}$ ,  $\mathbf{k} + \mathbf{n}_{14}$  and  $\mathbf{k} + \mathbf{n}_{19}$ . (b) When it is in region (a2), the polytope has five neighboring polytopes sharing the same interior points.

Now the condition that  $\mathbf{k}$  satisfies the mesh condition can be further simplified

by considering parallelepiped  $P(k_4, k_0, k_1)$  sandwiched between the six grid planes  $k_4 - 1, k_4, k_0 - 1, k_0, k_1 - 1$ , and  $k_1$ . Using (2) for the grid planes, we can solve for the points of intersections, and find that for every point  $\mathbf{r}$  in  $P(k_4, k_0, k_1)$ , we may write

$$\begin{aligned} K_0(\mathbf{r}) &= k_0, & K_1(\mathbf{r}) &= k_1, & K_2(\mathbf{r}) &= \lfloor \alpha \rfloor + k_4 + m, \\ K_3(\mathbf{r}) &= \lfloor \beta \rfloor + k_1 + n, & K_4(\mathbf{r}) &= k_4, \end{aligned} \quad (12)$$

where  $\lfloor x \rfloor$  is the greatest integer less or equal to  $x$ , while  $m$  and  $n$  are integers satisfying  $-1 \leq m, n \leq 2$ , and

$$\begin{aligned} \alpha &= p^{-1}(k_0 - k_1 - \gamma_0 + \gamma_1) + \gamma_2 - \gamma_4, \\ \beta &= p^{-1}(k_0 - k_4 - \gamma_0 + \gamma_4) + \gamma_3 - \gamma_1. \end{aligned} \quad (13)$$

The range of  $m$  and  $n$  in equation (12) is limited by their possible values at the eight corners of the parallelepiped, but not all 16 choices are allowed by the mesh condition. Therefore, we now project  $\mathbf{K}(\mathbf{r})$  given by (12) to  $\mathcal{D}$  and find

$$\mathbf{D}^T(\mathbf{K}(\mathbf{r}) - \boldsymbol{\gamma}) = \sum_{j=0}^4 (K_j(\mathbf{r}) - \gamma_j) \mathbf{d}_j = (m - a) \mathbf{d}_2 + (n - b) \mathbf{d}_3, \quad (14)$$

in which  $a \equiv \{\alpha\} \equiv \alpha - \lfloor \alpha \rfloor$  and  $b \equiv \{\beta\} \equiv \beta - \lfloor \beta \rfloor$ . The vector (14) must lie within the decagon  $\mathcal{Q}$ . Thus the allowed values of  $m$  and  $n$  are determined by  $a$  and  $b$  only. As the differences  $k_0 - k_4$  and  $k_0 - k_1$  run through all integer values, we find from Kronecker's theorem that  $a$  and  $b$  are everywhere dense and uniformly distributed in the interval  $(0, 1)$ .

Furthermore, because of the difference property shown in (13),  $\alpha$  and  $\beta$ , which determine the configuration of the parallelepiped, remain the same, if  $(k_0, k_1, k_4) \rightarrow (k_0 + \ell, k_1 + \ell, k_4 + \ell)$ . As a consequence we find  $\mathbf{K}(\mathbf{r}) \rightarrow \mathbf{K}(\mathbf{r}) + \ell \mathbf{n}_{31}$ , and its projection is periodic in the  $z$  direction with period equal to 5. It is also interesting to note that if  $\boldsymbol{\gamma} \rightarrow \boldsymbol{\gamma} - \frac{c}{5} \mathbf{n}_{31}$ ,  $\alpha$  and  $\beta$  in (13) are also unchanged, so that the projection into the 3d space does not show drastic changes when  $c \neq 0$ , which is behavior very different from the 2-d case [16].

It is not difficult to find values of  $(a - m, b - n)$  corresponding to the ten vertices of the decagon  $\mathcal{Q}$  given by (9). We find

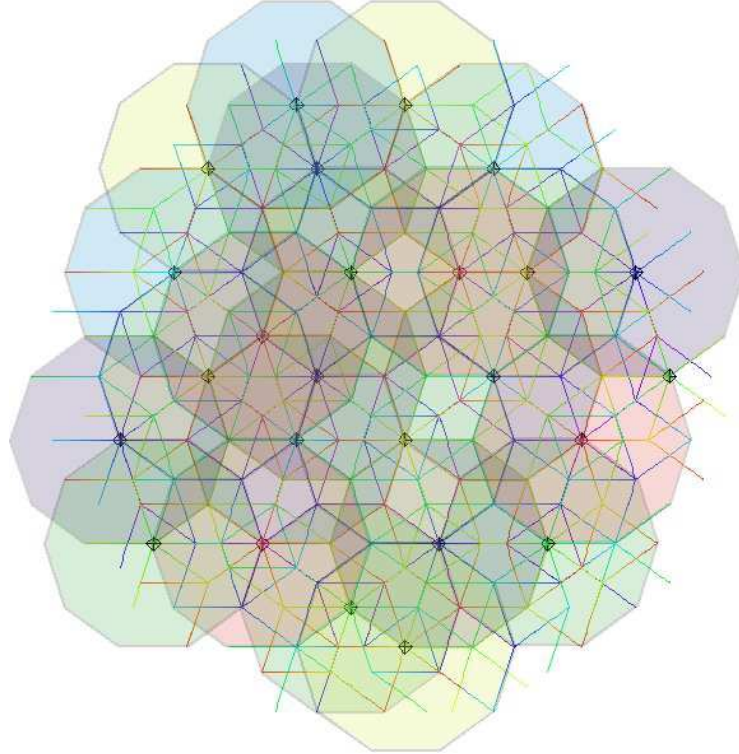


Fig. 3. The projection of  $\mathcal{L}$  in the  $xy$ -plane. Each polytope is represented by a decagon; its tip by a diamond. The bottoms of polytopes are at five different heights, and are represented by decagons of five different colors. Due to the difference in heights, the large overlapping area in the  $xy$ -projection, do not necessarily mean that the corresponding polytopes in 3d actually share a large volume.

$$\begin{aligned}
& \mathbf{Q}_{16} \leftrightarrow (a-0, b-0) = (1, 1), \quad \mathbf{Q}_{11} \leftrightarrow (a-0, b+1) = (0, p), \\
& \mathbf{Q}_{18} \leftrightarrow (a-1, b+1) = (-1, p), \quad \mathbf{Q}_{13} \leftrightarrow (a-2, b+1) = (-p, 1), \\
& \mathbf{Q}_{20} \leftrightarrow (a-2, b-0) = (-p, 0), \quad \mathbf{Q}_{15} \leftrightarrow (a-1, b-1) = (0, -1), \\
& \mathbf{Q}_{17} \leftrightarrow (a-1, b-2) = (0, -p), \quad \mathbf{Q}_{12} \leftrightarrow (a-0, b-2) = (1, -p), \\
& \mathbf{Q}_{19} \leftrightarrow (a+1, b-2) = (p, -1), \quad \mathbf{Q}_{14} \leftrightarrow (a+1, b-1) = (p, 0),
\end{aligned} \tag{15}$$

up to ambiguities when  $a$  or  $b$  is integer, as  $m$  or  $n$  changes by 1 when choosing  $a$  or  $b$  to be 0 or 1. The edges of decagon  $\mathbf{Q}$  lead to linear equations in  $(a-m, b-n)$  and the mesh condition for  $\mathbf{K}(\mathbf{r})$  becomes a set of inequalities in  $a-m$  and  $b-n$ . Hence, it is very easy to create a routine to generate  $\mathcal{L}$ .

Noting that  $\mathcal{L}$  is periodic in the  $z$ -direction, and aperiodic in the  $xy$ -directions, the projection of  $\mathcal{L}$  into the  $xy$ -plane is shown in Fig. 3, in which each decagon is the projection of a polytope  $\mathcal{P}$ , which overlaps with its neighbors.

Since real quasicrystals have icosahedra or triacontahedra as unit cells, which

are projections of a six-dimensional hypercube to a 3d space [9], the above method perhaps can also be used to determine all possible overlappings and their frequencies.

We are most thankful to Dr. M. Widom for providing us with many useful references.

## References

- [1] D. Shechtman, I. Blech, D. R. Gratias, and J. W. Cahn, *Metallic Phase with Long-Range Orientational Order and No Translational Symmetry*, Phys. Rev. Lett. **53** (1984) 1951–1953.
- [2] R. Penrose, *Tilings and Quasi-Crystals; a Non-Local Growth Problem?*, in *Introduction to The Mathematics of Quasicrystals*, Aperiodicity and Order, Vol. 2, M. V. Jarić, ed., (Academic Press, Boston, 1989), pp. 53–79.
- [3] B. Grünbaum and G. C. Shephard, *Tilings and Patterns*, (W. H. Freeman and Co., New York, 1987), Ch. 10.
- [4] N. G. de Bruijn, *Algebraic Theory of Penrose’s Non-Periodic Tilings of the Plane. I*, Indagationes Mathematicae **84** (1981) 38–52; —. *II*, ibid. **84** (1981) 53–66.
- [5] P. Gummelt, *Penrose Tilings as Coverings of Congruent Decagons*, Geometriae Dedicata **62** (1996) 1–17.
- [6] P. J. Steinhardt and H. C. Jeong, *A Simpler Approach to Penrose Tilings with implications for quasicrystal formation*, Nature **382** (1996) 433–435.
- [7] P. J. Steinhardt, H. C. Jeong, K. Saitoheong, M. Tanaka, E. Abe, and A. P. Tsai, *Experimental Verification of the Quasi-Unit-Cell Model of Quasicrystal Structure*, Nature **396** (1996) 55–57.
- [8] P. J. Lord and S. Ranganathan, *The Gummelt Decagon as a ‘Quasi Unit Cell’*, Acta Crystallogr. A **57** (2001) 531–539.
- [9] P. J. Lord, S. Ranganathan and U. D. Kulkarni, *Quasicrystals: Tiling versus Clustering*, Philosophical Magazine A **81** (2001) 2645–2651.
- [10] N. G. de Bruijn, *Quasicrystal and their Fourier transform*, Indagationes Mathematicae **89** (1986) 123–152.
- [11] F. Gähler and J. Rhyner, *Equivalence of the Generalised Grid and Projection Methods for the Construction of Quasiperiodic Tilings*, J. Phys. A **19** (1986) 267–277.
- [12] V. Elser, *The Diffraction Pattern of Projected Structures*, Acta Crystallogr. A **42** (1986) 36–43.

- [13] M. Duneau and A. Katz, *Quasiperiodic Patterns*, Phys. Rev. Lett. **54** (1985) 2688–2691.
- [14] A. L. Mackay, *Crystallography on the Penrose Pattern*, Physica A **114** (1982) 609–613.
- [15] M. Baake, D. Joseph, P. Kramer, and M. Schlottmann, *Root Lattices and Quasicrystals*, J. Phys. A **23** (1990) L1037–L1041.
- [16] H. Au-Yang and J. H. H. Perk, *Generalized Penrose Tiles*, to be published.
- [17] D. Levine and P. J. Steinhardt, *Quasicrystals. I. Definition and Structure*, Phys. Rev. B **34** (1986) 596–616.
- [18] J. E. S. Socolar and P. J. Steinhardt, *Quasicrystals. II. Unit-Cell Configurations*, Phys. Rev. B **34** (1986) 617–647.